Relationships Between Ψ_{B}-Energy Operator and Some Time-Frequency Representations

Abdel-Ouahab Boudraa, *Senior Member IEEE*

***Abstract*—Ψ_{B} operator is an energy operator that measures the interactions between two complex signals. In this letter, new properties of Ψ_{B} operator are presented. Connections between Ψ_{B} operator and some time-frequency representations (cross-ambiguity function, short-time Fourier transform, Zak transform, and Gabor coefficients are established. Link between Ψ_{B} operator of two input signals and their cross-spectrum is also derived. For two equal input signals, we fin that Fourier transform of Ψ_{B} operator is proportional to the second derivative of the ambiguity function. The established links show the ability of Ψ_{B} operator to analyze non stationary signals. A numerical example is provided for illustrating how to estimate the second order moment, of a FM signal, using Ψ_{B} operator. We compare the result to the moment given by the Wigner Ville distribution.**

***Index Terms*—Ψ_{B} energy operator, cross-ambiguity, short-time Fourier transform, Gabor coefficients cross-spectrum.**

I. Introduction

Ψ_{B} operator has been introduced to analyze the interaction between two signals [1]-[2]. This operator is an extension of the cross Teager-Kaiser operator [3] to deal with complex signals [1]. We have recently shown how Ψ_{B} operator can be used for segmentation of dynamic nuclear cardiac images [4], transient detection [5], time delay estimation [6] and time series analysis [7]. Ψ_{B} operator is define by [1]:

$$\begin{aligned}\Psi_{\mathrm{B}}(x(t),y(t)) &= [0.5\dot{x}(t)\dot{y}^*(t) - 0.25(\ddot{x}(t)y^*(t) + x(t)\ddot{y}^*(t))] \\ &+ [0.5\dot{x}^*(t)\dot{y}(t) - 0.25(\ddot{x}^*(t)y(t) + x^*(t)\ddot{y}(t))]\end{aligned} \tag{1}$$

Let $R_{xy}(t,\tau)$ be the instantaneous Cross Correlation (CC) of $x(t)$ and $y(t)$:

$$R_{xy}(t,\tau) = x(t+\frac{\tau}{2}).y^*(t-\frac{\tau}{2}) \tag{2}$$

The output of Ψ_{B} is related to $R_{xy}(t,\tau)$ as follows [1]:

$$\Psi_{\mathrm{B}}(x(t),y(t)) = -\frac{\partial^2 R_{xy}(t,\tau)}{\partial\tau^2}\bigg|_{\tau=0} - \frac{\partial^2 R^*_{xy}(t,\tau)}{\partial\tau^2}\bigg|_{\tau=0} \tag{3}$$

For $x(t) = y(t)$ the notation $\Psi_{\mathrm{B}}(x(t),y(t)) \equiv \Psi_{\mathrm{B}}(x(t))$ is used. Examination of Eq. (3) shows that Ψ_{B} is a cross-energy function of two signals. Thus, links to transforms using the concept of instantaneous CC, such as Time-Frequency Representations (TFRs), can be found. In this letter new properties of Ψ_{B} are introduced. We show how some TFRs (Gabor Coefficient (GC), Short-Time Fourier Transform (STFT), Ambiguity Function (AF), and Zak Transform (ZT)) which are fundamentally similar and their application domains quite different, are related to Ψ_{B}. These links show that Ψ_{B} can be useful for non stationary signals analysis.

A.O. Boudraa is with IRENav, Ecole Navale, BCRM Brest, CC 600, 29240 BREST Cedex 9, France. e-mail: boudra@ecole-navale.fr.

II. Short-Time Fourier Transform

STFT is a classical TFR which allows one to obtain localized information of time and frequency of a signal. This transform is constructed by firs choosing an analysis window, $x^*(t-a)$, and then compute the Fourier Transform (FT) of the windowed signal $y(t)$ [8]:

$$\psi_{xy}(a,b) = \int y(t)x^*(t-a)e^{-2j\pi tb}dt \tag{4}$$

where a and b are the delay and the modulation parameters. To relate Ψ_{B} to STFT, we recall the link between Ψ_{B} and the cross Wigner-Ville Distribution (WVD)[1], $W_{xy}(t,\nu)$ [1]:

$$\Psi_{\mathrm{B}}(x(t),y(t)) = 4\pi^2\int \nu^2(W_{xy}(t,\nu) + W^*_{xy}(t,\nu))d\nu \tag{5}$$

$$\text{where} \quad W_{xy}(t,\nu) = \int R_{xy}(t,\tau)e^{-2j\pi\nu\tau}d\tau \tag{6}$$

Let $x(t)$ and $y(t)$ be two complex signals. Ψ_{B} is linked to STFT by

$$\begin{aligned}\Psi_{\mathrm{B}}(x(t),y(t)) &= 8\pi^2\int \nu^2\big[\psi_{y\_x}(2t,2\nu) + \psi_{y^*_-x^*}(2t,2\nu)\big] \\ &\times\ e^{4j\pi\nu t}d\nu\end{aligned} \tag{7}$$

where $y_-(t') = y(-t')$

Proof: We set $u = t + \tau/2$ in (6) and we obtain

$$W_{xy}(t,\nu) = 2e^{4j\pi\nu t}\int x(u)y^*(2t-u)e^{-2j\pi u(2\nu)}du \tag{8}$$

If we set $y_-(t') = y(-t')$, Eq. (8) simplifie to

$$W_{xy}(t,\nu) = 2e^{4j\pi\nu t}\psi_{y\_x}(2t,2\nu) \tag{9}$$

Using the same setting and the conjugate version of Eq. (6) we obtain

$$W_{x^*y^*}(t,\nu) = 2e^{4j\pi\nu t}\psi_{y^*_-x^*}(2t,2\nu) \tag{10}$$

Summing Eqs. (9) and (10) and using Eq. (5) complete the proof. For $x(t) = y(t)$ being real signals, Eq. (7) is reduced to

$$\Psi_{\mathrm{B}}(x(t)) = 16\pi^2\int \nu^2\psi_{x\_x}(2t,2\nu)e^{4j\pi\nu t}d\nu \tag{11}$$

Equations (7) and (11) show that time resolution changes by a factor of 2. Thus, spacing of Ψ_{B} is quite large compared to the range of evaluation points for the STFT. Since the second order moment does not have a scaling factor in time and frequency, a well define sampling grid must be used. If νt is integer, Eq. (11) is reduced to Eq. (12) which corresponds to the second

[1]All integrals are from $-\infty$ to $+\infty$ unless otherwise stated.

order moment in frequency of the STFT where the window is chosen to be the time-reversed input signal.

$$\Psi_{\rm B}(x(t/2)) = 2\pi^2 \int (-1)^{\nu t}\nu^2 \psi_{x\_x}(t,\nu)d\nu \qquad (12)$$

III. Gabor Coefficients

GC is a signal analysis tool, for example, to process textured images. Using an analyzing function, $\gamma(t)$, and for a given input signal $f(t)$, GC are define as follows [9]:

$$C_{m,n} = \int f(t+n)\gamma^*(t)e^{-2j\pi mt}dt \qquad (13)$$

Let $x(t)$ and $y(t)$ be two complex signals. $\Psi_{\rm B}$ operator is related to GC by

$$\Psi_{\rm B}(x(t),y(t)) = 8\pi^2 \int \nu^2 \big[C_{2\nu,2t} + C^*_{-2\nu,2t}\big]e^{-4j\pi\nu t}d\nu \qquad (14)$$

where $\gamma(t') = y(-t')$

Proof: Using the same reasoning as for the STFT with $u = \tau/2 - t$ we have

$$W_{xy}(t,\nu) = 2e^{-4j\pi\nu t}C_{2\nu,2t} \qquad (15)$$

$$W_{x^*y^*}(t,\nu) = 2e^{-4j\pi\nu t}C^*_{-2\nu,2t} \qquad (16)$$

Summing Eqs. (15) and (16) and using relation (5), we derive the relation (14). If the signal is sampled in both time and frequency with well define sampling grid such that $m = 2\nu$ and $n = 2t$, we can rewrite (14) as

$$\begin{aligned}\Psi_{\rm B}(x(t),y(t)) &= 8\pi^2 \int \nu^2 \big[C_{2\nu,2t} + C^*_{-2\nu,2t}\big]d\nu \\ \Psi_{\rm B}(x(\tfrac{n}{2}),y(\tfrac{n}{2})) &\approx 2\pi^2 \sum_m (-1)^{mn}m^2\big[C_{m,n} + C^*_{-m,n}\big] \qquad (17)\end{aligned}$$

For $x(t) = y(t)$ being real signals, relation (17) is reduced to

$$\Psi_{\rm B}(x(t)) = 16\pi^2 \int \nu^2 C_{2\nu,2t}d\nu \qquad (18)$$

$$\Psi_{\rm B}(x(\frac{n}{2})) \approx 4\pi^2 \sum_m (-1)^{mn}m^2 C_{m,n} \qquad (19)$$

Spacing of $\Psi_{\rm B}$ is quite large compared to the range of evaluation points for GC. Equation (18) shows that $\Psi_{\rm B}$ corresponds to the second order moment of GC. The spacing of the GC and the STFT are large compared to the range of evaluation points for $\Psi_{\rm B}$. This has a direct effect on the application for which each is best suited. Both the GC and the STFT are useful where there is a large amount of data, which must be analyzed at some coarser resolution (some feature extraction task as part of a larger image analysis problem). Thus, in this case $\Psi_{\rm B}$ is an efficien and a simple way to calculate the second moment in frequency of both the GC or the STFT.

IV. Cross Ambiguity Function

Cross AF (CAF) is a TFR that is useful in many signal communication systems. CAF is given by:

$$A_{xy}(u,\tau) = \int R_{xy}(t,\tau)e^{-j2\pi ut}dt \qquad (20)$$

Let $\Gamma_{xy}(u,\nu)$ be the FT, $\mathcal{F}$, of $A_{xy}(u,\tau)$ with respect to τ

$$R_{xy}(t,\tau) \overset{t}{\longleftrightarrow} A_{xy}(u,\tau) \overset{\tau}{\longleftrightarrow} \Gamma_{xy}(u,\nu) \qquad (21)$$

$\Gamma_{xy}(u,\nu)$ represents the 2D FT of $R_{xy}(t,\tau)$ and is the cross spectrum of $x(t)$ and $y(t)$. $A_{xy}(u,\tau)$ is expressed in terms of the FTs $X(\nu)$ and $Y(\nu)$ of $x(t)$ and $y(t)$ respectively as

$$\begin{aligned}A_{xy}(u,\tau) &= \int \Gamma_{xy}(u,\nu)e^{j2\pi\tau\nu}d\nu \\ &= \int X(\nu+\frac{u}{2})Y^*(\nu-\frac{u}{2})e^{j2\pi\tau\nu}d\nu \qquad (22)\end{aligned}$$

Let $x(t)$ and $y(t)$ be two complex signals. $\Psi_{\rm B}$ is related to $\Gamma_{xy}(u,\nu)$ by

$$\mathcal{F}\{\Psi_{\rm B}(x(t),y(t))\}(u) = 4\pi^2 \int \nu^2\big[\Gamma_{xy}(u,\nu) + \Gamma^*_{xy}(-u,-\nu)\big]d\nu \qquad (23)$$

Proof: According to Eq. (21), $R_{xy}(t,\tau)$ can be rewritten as

$$R_{xy}(t,\tau) = \iint \Gamma_{xy}(u,\nu)e^{j2\pi(ut+\nu\tau)}dud\nu \qquad (24)$$

Differentiating twice both sides of $R_{xy}(t,\tau)$ and $R^*_{xy}(t,\tau)$ with respect to τ one gets

$$\begin{aligned}\frac{\partial^2 R_{xy}(t,\tau)}{\partial\tau^2}\bigg|_{\tau=0} &= -4\pi^2 \iint \nu^2\Gamma_{xy}(u,\nu)e^{j2\pi ut}dud\nu \qquad (25)\\ \frac{\partial^2 R^*_{xy}(t,\tau)}{\partial\tau^2}\bigg|_{\tau=0} &= -4\pi^2 \iint \nu^2\Gamma^*_{xy}(-u,-\nu)e^{j2\pi ut}dud\nu \qquad (26)\end{aligned}$$

Summing Eqs. (25) and (26) and using Eq. (3) followed by the FT complete the proof. Let $x(t)$ and $y(t)$ be two complex signals. The FT of $\Psi_{\rm B}$ operator is linked to CAF by

$$\mathcal{F}\{\Psi_{\rm B}(x(t),y(t))\}(u) = -\frac{\partial^2}{\partial\tau^2}\Big[A_{xy}(u,\tau) + A^*_{xy}(-u,\tau)\Big]_{\tau=0} \qquad (27)$$

Proof: According to Eq. (20) $R_{xy}(t,\tau)$ can be written as

$$R_{xy}(t,\tau) = \int A_{xy}(u,\tau)e^{j2\pi ut}du \qquad (28)$$

Differentiating twice both sides of Eq. (28) and its conjugate version we get

$$\begin{aligned}\frac{\partial^2 R_{xy}(t,\tau)}{\partial\tau^2}\bigg|_{\tau=0} &= \int \frac{\partial^2 A_{xy}(u,\tau)}{\partial\tau^2}\bigg|_{\tau=0} e^{j2\pi ut}du \qquad (29)\\ \frac{\partial^2 R^*_{xy}(t,\tau)}{\partial\tau^2}\bigg|_{\tau=0} &= \int \frac{\partial^2 A^*_{xy}(-u,\tau)}{\partial\tau^2}\bigg|_{\tau=0} e^{j2\pi ut}du \qquad (30)\end{aligned}$$

Using Eq. (3) we obtain

$$\begin{aligned}\Psi_{\rm B}(x(t),y(t)) &= -\int \underbrace{\frac{\partial^2}{\partial\tau^2}\Big[A_{xy}(u,\tau) + A^*_{xy}(-u,\tau)\Big]_{\tau=0}}_{H(u)} \\ &\times\ e^{j2\pi ut}du \qquad (31)\end{aligned}$$

Observe from Eq. (31) that Ψ_{B} is the inverse FT of $H(u)$. Let $x(t)$ and $y(t)$ be two complex signals. If $x(t) = y(t)$ then

$$\mathcal{F}\{\Psi_{\mathrm{B}}(x(t))\}(u) = -2\frac{\partial^2 A_{xx}(u,\tau)}{\partial\tau^2}\bigg|_{\tau=0} \qquad (32)$$

Proof: Using Eq. (2) it is easy to see that for $x(t) = y(t)$

$$\frac{\partial^2 R_{xx}(t,\tau)}{\partial\tau^2}\bigg|_{\tau=0} = \frac{\partial^2 R^*_{xx}(t,\tau)}{\partial\tau^2}\bigg|_{\tau=0} \qquad (33)$$

and it follows from (29) and (30) that

$$\frac{\partial^2 A_{xx}(u,\tau)}{\partial\tau^2}\bigg|_{\tau=0} = \frac{\partial^2 A^*_{xx}(-u,\tau)}{\partial\tau^2}\bigg|_{\tau=0} \qquad (34)$$

Using Eq. (31) with $x(t) = y(t)$ one gets

$$\int \Psi_{\mathrm{B}}(x(t))e^{-j2\pi ut}dt = -2\frac{\partial^2 A_{xx}(u,\tau)}{\partial\tau^2}\bigg|_{\tau=0} \qquad (35)$$

which completes the proof.

Computing the FT of Ψ_{B} is identical to computing the second derivative, with respect to lag τ, of the CAF. Equation (23) shows another link of the FT of Ψ_{B} which is equal to the second order moment in frequency of the cross spectrum of the two input signals. Eq. (32) gives the link between Ψ_{B} and the AF.

V. Zak Transform

ZT is a mixed TFR of a signal that has relationships with the WVD, the Rihaczek distribution, and the Radar AF [10]. For $\alpha \geq 0$, ZT of f, $Z_\alpha f$, is a function on $\mathbb{R}^{2d}$:

$$Z_\alpha f(x,y) = \sum_{k\in\mathbb{Z}} f(x-\alpha k)e^{-2j\pi\alpha ky} \qquad (36)$$

In this work, we use the ZT with $\alpha = 1$, $d = 1$, which is denoted by $Z_f(x,y)$. The CAF of $f(t)$ and $g(t)$ can be computed directly from ZTs $Z_f(x,y)$ and $Z_g(x,y)$:

$$A_{fg}(u,\tau) = \int_0^1\int_0^1 Z_f(x,y)Z^*_g(x+\tau,y+u)e^{-2j\pi xu}dxdy \qquad (37)$$

Let $f(t)$ and $g(t)$ be two complex signals. Ψ_{B} is related to the ZT by

$$\Psi_{\mathrm{B}}(f(t),g(t)) = \int_{-\infty}^{+\infty}\int_0^1\int_0^1 (Z_f(x,y)\ddot{Z}^*g(x,y+u) + Z^*_f(x,y)\ddot{Z}_g(x,y-u))e^{-2j\pi u(x-t)}dxdydu \qquad (38)$$

Proof: Differentiating twice both sides of equation (37) and its conjugate version with respect to τ we get

$$\frac{\partial^2 A_{fg}(u,\tau)}{\partial\tau^2}\bigg|_{\tau=0} = \int_0^1\int_0^1 Z_f(x,y)\ddot{Z}^*_g(x,y+u)e^{-2j\pi xu}dxdy \qquad (39)$$

$$\frac{\partial^2 A^*_{fg}(u,\tau)}{\partial\tau^2}\bigg|_{\tau=0} = \int_0^1\int_0^1 Z^*_f(x,y)\ddot{Z}_g(x,y-u)e^{-2j\pi xu}dxdy \qquad (40)$$

Substituting Eqs. (39) and (40) in Eq. (31) completes the proof where $\ddot{Z}_g(x,y+u) = \partial^2 Z_g(x+\tau,y\pm u)/\partial\tau^2|_{\tau=0}$. If $f(t) = g(t)$, equation (38) is reduced to

$$\Psi_{\mathrm{B}}(f) = 2\int_{-\infty}^{+\infty}\int_0^1\int_0^1 Z_f(x,y)\ddot{Z}^*g(x,y+u)e^{-2j\pi u(x-t)}dxdydu \qquad (41)$$

The AF on the integer lattice is define as

$$A_{ff}(n,m) = \int_0^1\int_0^1 \mid Z_f(x,y)\mid^2 e^{2j\pi(-mx+ny)}dxdy \qquad (42)$$

Using equation (32) it is easy to show that

$$\mathcal{F}\{\Psi_{\mathrm{B}}(x(t))\}(n) = 8\pi^2\int_0^1\int_0^1 x^2(t)\mid Z_f(x,y)\mid^2 e^{2j\pi ny}dxdy \qquad (43)$$

Eqs. (38), (41), and (43) reveals links between ZT and Ψ_{B}.

VI. Results

We show how Ψ_{B} can be used to estimate the second order moment in frequency, $<\nu^2>_t$, of an FM signal, which is a useful feature for signal classification Using equation (5), the moment $<\nu^2>_t$ of signal $y(t)$ is given by

$$<\nu^2>_t = \frac{\int \nu^2 W_y(t,\nu)d\nu}{\mid y(t)\mid^2} \qquad (44)$$

$$<\nu^2>_t = \frac{\Psi_{\mathrm{B}}(y(t))}{8\pi^2\mid y(t)\mid^2} \qquad (45)$$

where $\mid y(t)\mid^2 = \int W_y(t,\nu)d\nu$. Let $y(t)$ be a noisy version of LFM signal, $x(t) = e^{2j\pi\phi(t)}$, define by

$$y(t) = x(t) + n(t) \qquad (46)$$

$\phi(t) = \alpha t^2 + \beta t + c$. $n(t)$ is a Gaussian noise, $\mathcal{N}(0,\sigma^2)$. This complex noise consists of independent real and imaginary parts. The WVD of $x(t)$ is a Dirac function concentrated along its instantaneous frequency, $\nu_x(t) = 2\alpha t + \beta$:

$$W_x(t,\nu) = \delta(\nu - \beta - 2\alpha t) \qquad (47)$$

Since $\mid x(t)\mid^2 = 1$ and putting (47) in Eq. (44) we obtain

$$<\nu^2>_t = (2\alpha t + \beta)^2 \qquad (48)$$

To illustrate the computation of $<\nu^2>_t$, we consider a signal $y(t)$ with parameters ($\alpha = 50, \beta = 25, c = 10$) where $t \in [0, 1.2]$, sampled at $T = 5.10^{-4}$ and with different SNRs. We compare the true value of $<\nu^2>_t$ (Eq. 48) and the numerical estimations by WVD (Eq. 44) and Ψ_{B} (Eq. 45). Operator Ψ_{B} is implemented using symmetric finit difference scheme [6]. WVD displayed in Fig. 1, clearly reveals the features of the noisy signal $y(t)$ (SNR=40 dB). Results of $<\nu^2>_t$, by Ψ_{B} and WVD, from 600 runs Monte-Carlo simulations are shown in Figs. 2 and 3. Origin of time axis is shifted to -0.1 sec for displaying purpose. Although the match of the moments $<\nu^2>_t$ is not perfect, Ψ_{B} shows a good match (Fig. 2) and with little oscillations due to noise (Fig. 3(a)). Figure 2 also shows an agreement of the WVD moment with the true value but with fluctuation of high magnitude at the beginning and the end of free-noise signal $x(t)$. These fluctuation are due to the effect of the broad frequency spread observed on the beginning and on the end of the signal $y(t)$ (Fig. 1). For noisy signal, these fluctuation are very high over all the signal (Fig. 3(b)). In Fig. 4(a), we plot the MSEs in $<\nu^2>_t$ estimation versus the SNRs for both $\Psi_{\rm B}$ and VWD. As seen in Fig. 4(a), across a range of different SNRs, $\Psi_{\rm B}$ provides a good performance over the VWD. Bias measures reported in Fig. 4(b) show that both $\Psi_{\rm B}$ and WVD are less biased for SNR $>$ 15 dB but the little bias is achieved by DWV. Due to its localization property, $\Psi_{\rm B}$ is sensitive in very noisy environment compared to WVD, however it offers a significan computation advantage over WVD. Cost of calculating $\Psi_{\rm B}$ is very small compared to WVD. In general, $\Psi_{\rm B}$ gives interesting results provided that $\Psi_{\rm B}(n(t)) \simeq -2\Psi_{\rm B}(x(t), n(t))$. Also, attention must be given to discretization of $\Psi_{\rm B}$.

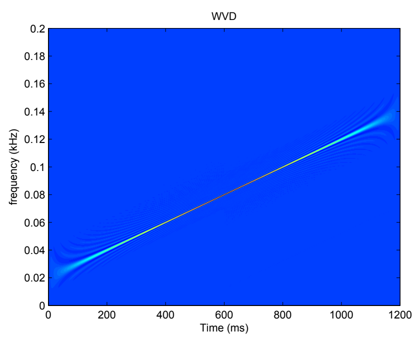

Fig. 1. WVD of noisy signal $y(t)$ (SNR=40dB).

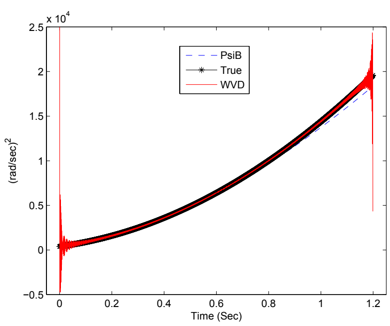

Fig. 2. Moment $<\nu^2>_t$ of $y(t)$ (SNR=∞). True (black star), $\Psi_{\rm B}$ (blue dashed line) and WVD (red solid line).

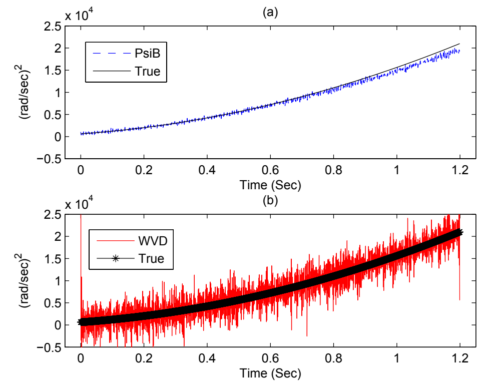

Fig. 3. Moment $<\nu^2>_t$ of $y(t)$ (SNR=40 dB). True (black), $\Psi_{\rm B}$ (blue dashed line) and WVD (red solid line).

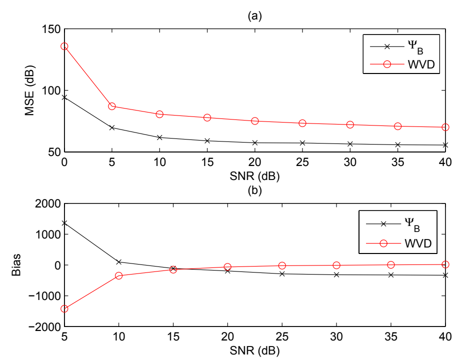

Fig. 4. (a): MSEs (dB) in $<\nu^2>_t$ estimation for $\Psi_{\rm B}$ and WVD. (b): Bias in $<\nu^2>_t$ estimation for $\Psi_{\rm B}$ and WVD.

VII. Concluding Remarks

Main point of this letter is to establish links between $\Psi_{\rm B}$ and some TFRs. Even the studied TFRs have different application domains, they are all related to $\Psi_{\rm B}$. Lemmas 1 and 2 show that time resolution changes by a factor of 2. Thus, the spacing of $\Psi_{\rm B}$ is quite large compared to the range of evaluation points for both STFT and GC. Connections between ZT and $\Psi_{\rm B}$ are also derived. The established links show the interest of $\Psi_{\rm B}$ to analyze non stationary signals. Particularly relation (18) shows that $\Psi_{\rm B}$ corresponds to the second order moment in frequency of GC. We have established the link between the FT of $\Psi_{\rm B}$ of two input signals and the second order moment of the cross-spectrum. For two equal input signals we fin that the FT of $\Psi_{\rm B}$ is proportional to the second derivative of the AF. Preliminary results show that in moderate noisy environment $\Psi_{\rm B}$ is effective for estimating the second order frequency moment of a signal.

References

[1] J.C. Cexus and A.O. Boudraa, "Link between cross-Wigner distribution and cross-Teager energy operator," *IEE Elec. Lett.,* vol. 40, no. 12, pp. 778-780, 2004.

[2] A.O. Boudraa, J.C. Cexus, K. Abed-Meraim and Z. Saidi, "Interaction measure of AM-FM signals by cross-$\Psi_{\rm B}$-energy operator," *Proc. IEEE ISSPA,* pp. 775-778, 2005.

[3] J.F. Kaiser, "Some useful properties of Teager's energy operators" *Proc. ICASSP,* vol. 3, pp. 149-152, 1993.

[4] A.O. Boudraa, J.C. Cexus and H. Zaidi, "Functional segmentation of dynamic nuclear medicine images by cross-$\Psi_{\rm B}$-energy operator," *Comput. Meth. Prog. BioMed.,* vol. 84, no 2-3, pp 146-152, 2006.

[5] A.O. Boudraa, S. Benramdane, J.C. Cexus and T. Chonavel, "Some useful properties of cross-$\Psi_{\rm B}$-energy operator," *International Journal of Electronics and Communications*, vol. 63, issue 9, pp. 728-735, 2009.

[6] A.O. Boudraa, J.C. Cexus and K. Abed-Meraim, "Cross-$\Psi_{\rm B}$-energy operator-based signal detection," *Journal of Acoustical Society of America,* vol. 123, no. 6, pp. 4283-4289, 2008.

[7] A.O. Boudraa, J.C. Cexus, M. Groussat and P. Brunagel, "An energy-based similarity measure for time series," *Advances in Signal Processing,* ID 135892, 8 pages, 2008.

[8] A. Mertins, *Signal Analysis: Wavelets, Filter Banks, Time-Frequency Transforms and Applications*, John Wiley-Sons., Chichester, 1999

[9] M.J. Bastiaans, "Gabor's signal expansion and its relation to sampling of the sliding-window spectrum," in *Advanced Topics in Shannon Sampling and Interpolation Theory*, R.J. Marks II, ed., Springer, pp. 1-37, 1993.

[10] A.J.E.M. Janssen, "The Zak transform: A signal transform for sampled time-continuous signals," *Philips J. Res.,* vol. 43, pp. 23-69, 1995.